Mössbauer study of hydrogenated amorphous germaniumtin thinfilm alloys

I. Chambouleyron, F. C. Marques, P. H. Dionisio, I. J. R. Baumvol, and R. A. Barrio

Citation: Journal of Applied Physics **66**, 2083 (1989); doi: 10.1063/1.344301
View online: http://dx.doi.org/10.1063/1.344301
View Table of Contents: http://scitation.aip.org/content/aip/journal/jap/66/5?ver=pdfcov
Published by the AIP Publishing

Mössbauer study of hydrogenated amorphous germanium-tin thin-film alloys

I. Chambouleyron and F. C. Marques
Instituto de Fisica, Universidade Estadual de Campinas, P. O. Box 6165, Campinas, S. P. 13081, Brazil

P. H. Dionisio and I. J. R. Baumvol
Instituto de Fisica, Universidade Federal de Rio Grande do Sul, Porto Alegre, R. S. 90049, Brazil

R. A. Barrio
Instituto de Investigacion en Materiales, Universidad Nacional Autonoma de Mexico, 04510 Mexico D. F., Mexico

(Received 12 September 1988; accepted for publication 21 April 1989)

This work reports on the structure of defects around Sn atoms in amorphous germanium-tin alloys deposited by the rf sputtering of compound targets. The influence of atomic hydrogen on the structure of such defects is reported for the first time. The samples were analyzed by Rutherford backscattering spectrometry and conversion electron Mössbauer spectroscopy. The main conclusion of this research is that, besides the known substitutional position of Sn atoms in the *a*-Ge network, a new Sn bonding configuration appears, which may be at the origin of the degradation of the optoelectronic properties of the alloy found experimentally. This new configuration is an octahedrally coordinated Sn atom resulting from the trapping of Ge vacancies by Sn atoms, the energetically favored final site being the tin atom in the center of the Ge relaxed divacancy.

I. INTRODUCTION

The optical properties of amorphous semiconductor alloys can be easily tailored by varying their composition. This characteristic is important for potential applications in the fields of solar energy conversion, imaging devices, and electrophotography. The optical band gap of hydrogenated amorphous silicon (*a*-Si:H), for instance, can be adjusted up to several eV by the incorporation of carbon or nitrogen into the network.[1] A similar situation is found to happen with *a*-Ge:H.[2,3] Amorphous Si-Ge alloys possess optical properties intermediate between those corresponding to both elemental semiconductors.[4] In the narrow-band-gap amorphous semiconductor family, some work has been done on *a*-Si:Sn:H.[5] However, the retention of good electronic properties for these alloys appears to be a more difficult task. Past experience shows that the addition of any foreign atom to the amorphous network of elemental semiconductors generally results in the degradation of photoconductivity. In all cases the transport properties of the alloys worsen as the foreign element content increases. The understanding and eventual mastering of this degradation problem has retained the attention of most workers in the field. The long-term prospects of the amorphous semiconductor technology rely partially on their success.

The optical properties of unhydrogenated amorphous Ge-Sn alloys prepared at low temperature were reported by Temkin, Connel, and Paul.[6] In previous publications the present authors discussed the structure and composition of unhydrogenated *a*-Ge-Sn films[7] and the semiconductor properties of hydrogenated germanium-tin alloys[8] deposited at 180 °C.

The main findings of Refs. 7 and 8 are the following.

(1) Stable Ge-Sn solid amorphous solutions with Sn concentrations ranging from 0 to nearly 30 at. % can be prepared onto glass substrates held at 180 °C.

(2) Under the preparation conditions reported in Refs. 7 and 8, almost all Sn atoms appear to bond to four Ge atoms in a covalent tetrahedral configuration, i.e., in a substitutional way.

(3) The incorporation of Sn atoms into the *a*-Ge network narrows the band gap at a rate of approximately -12 meV/at. % tin. Conversely, the addition of hydrogen widens the optical band gap, as expected. In hydrogenated samples a concomitant Ge dangling bond passivation mechanism is found to occur.

(4) The hydrogenated samples show an activated-type dark conductivity, the value of the activation energy depending on the tin and on the hydrogen content. On the contrary, the *a*-Ge:Sn films present a dark conductivity-versus-temperature behavior typical of electronic conduction through localized states or through impurity bands in the pseudogap. Infrared transmission spectra of alloyed samples indicate that hydrogen atoms bond only to Ge orbitals. No Sn-H vibrations were detected in the 400–4000-cm^{-1} wave-number range.

(5) Under air mass 1 (AM1) irradiation conditions, no photoconductivity was detected in hydrogenated samples containing Sn, an indication that the incorporation of tin in the network produces an exceedingly important density of defects. This experimental finding suggests that, in spite of Sn being an isoelectronic impurity in the Ge network, its presence induces new electronic states in the pseudogap, which may originate from Ge or Sn dangling bonds or from a new bonding configuration of the tin atoms. The possibility of having interstitial Sn atoms can be excluded, considering the relative sizes of germanium and tin atoms.

(6) Depending on the deposition temperature, metallic segregation may occur. At a substrate temperature of 180 °C the segregation process appears for tin concentrations above around 20 at. %. The study proved that the process is en-

 0021-8979/89/172083-08$02.40

hanced, in all cases, by the presence of hydrogen in the reaction chamber.

In this paper we present results on Mössbauer spectroscopy aiming at the identification of the structure of defects around tin atoms in *a*-Ge:Sn and *a*-Ge:Sn:H alloys. The present data indicate a new Sn bonding configuration in the Ge network which may originate the increased density of electronic states in the band gap found experimentally. This new configuration is an octahedrally coordinated Sn atom resulting from the trapping of Ge vacancies by Sn atoms, the energetically favored final site being the tin atom in the center of a relaxed Ge divacancy.

II. EXPERIMENT AND RESULTS

The samples discussed here were prepared onto substrates held at 180 °C by rf sputtering compound targets in an argon (and hydrogen) atmosphere. The details of preparation conditions can be found in Ref. 8. Each sample is labeled by a number and by the indication of the nature of the substrate supporting the film, i.e., intrinsic crystalline silicon (Si) or Corning 7059 glass (*g*). Both kinds of substrates were used in every deposition run. Table I shows the composition and general characteristics of the *a*-Ge:Sn samples being discussed here. In the present paper we maintain the sample labeling of Ref. 8, identical numbers meaning similar deposition conditions. The *a*-Ge:Sn and *a*-Ge:Sn:H samples were characterized by means of Rutherford backscattering (RBS) and conversion electron Mössbauer (CEMS) spectroscopies. The RBS analyses were performed with a 760-keV $^4He^{2+}$ beam from the Porto Alegre (Brazil) ion implanter. The overall resolution of the RBS spectrometer was 14 keV. The CEMS spectra were obtained in a backscattering geometry by mounting the samples on the backplate of a proportional counter through which He + 5% CH_4 was allowed to flow. Measurements were taken with the sample and source at room temperature. A conventional constant-acceleration Mössbauer spectrometer was used. The Mössbauer source used was ^{119m}Sn in $BaSnO_3$. The isomer shifts are quoted with respect to this source.

Figures 1 and 2 show the Rutherford backscattering spectra of the germanium-tin alloy samples listed in Table I. In Fig. 1 the RBS spectrum of a pure *a*-Ge sample [02(*g*)] is also given for comparison. The spectra of Fig. 1 do not indicate any metallic segregation at the surface of films having up to 15 at. % Sn, irrespective of the presence or absence of hydrogen in the reaction chamber. In Fig. 2 the RBS spectra of samples having higher Sn content are plotted. Two kinds of spectra are clearly seen. The spectrum of sample 09(*g*), i.e., 27 at. % tin on a glass substrate, does not indicate any metal segregation at the surface. If, under the same deposition conditions (in fact the same run), a crystalline silicon substrate is used [No. 09(Si)], the RBS spectrum show a shoulder in the tin signal, an indication of metallic segregation at the surface of the layer. Similar effects are measured in films deposited onto glass substrates if hydrogen is allowed to flow in the reactor chamber during the deposition

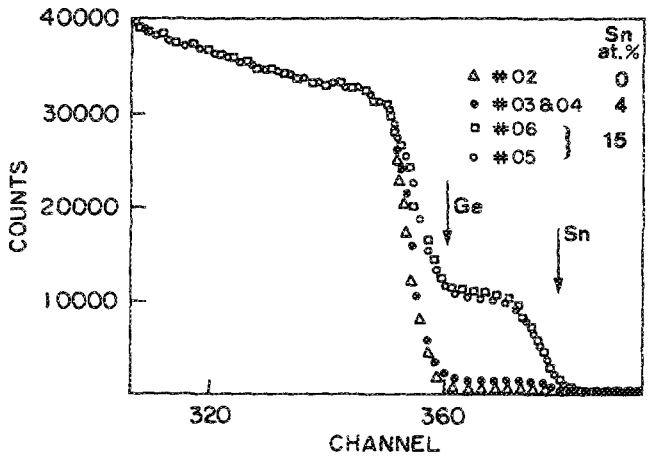

FIG. 1. Rutherford backscattering spectra from sputtered *a*-Ge, *a*-Ge:Sn, and *a*-Ge:Sn:H homogeneous alloys (up to Sn/(Ge + Sn) ~0.15) deposited onto Corning 7059 glass and crystalline silicon substrates. The incident α-particle beam energy and spectrometer resolution are 760 and 14 keV, respectively. The vertical arrows indicate the position in the RBS spectra of Sn and Ge at the surface.

TABLE I. Composition, hydrogen content, and metal segregation for some rf-sputtered *a*-Ge:Sn and *a*-Ge:Sn:H samples.

Sample No.	Tin (at. %) (a)	Tin (at. %) RBS	Hydrogen (at. %)	Observations
02	0	0	14	*a*-Ge:H (Ref. 19)
04	1	4	9	No Sn segregation
05	10	15	0	No Sn segregation
06	10	15	5	No Sn segregation
09(*g*)	20	27	0	No Sn segregation
09(Si)	20	···	0	β-Sn segregated
10(*g*)	20	···	yes	β-Sn segregated at the surface

[a] Estimated from sputtering yield and metallic target coverage.

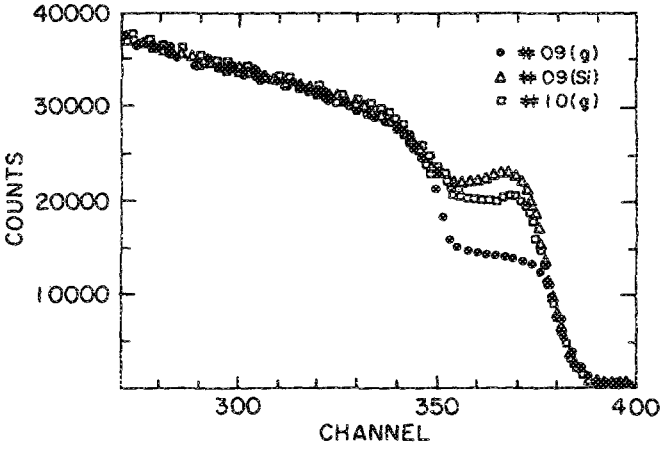

FIG. 2. Rutherford backscattering spectra of *a*-Ge:Sn and *a*-Ge:Sn:H showing a metal segregation at the outer surface. The spectrum of sample 09(*g*) (Sn/(Ge + Sn) ~0.27) showing no metallic segregation is also displayed. Measuring conditions are identical to those of Fig. 1.

process [No. 10 (g)]. In both cases the decrease of the RBS signal at a certain depth indicates the end of the segregation process and the appearance of an alloyed Ge:Sn layer. The segregated metal is β-Sn as indicated by x-ray diffraction data.[8]

Figures 3 and 4 and Table II show the Mössbauer spectra and the corresponding fitting parameters of samples 05(g), 06(g), 09(g), 09(Si), and 10(g). The data include hydrogenated, unhydrogenated, Sn-segregated, and nonsurface-segregated samples of different compositions.

The best fit to the Mössbauer spectra of the samples shown in Fig. 3 is obtained with a single Lorenzian. (The present authors are aware that the peaks may not be strictly Lorenzians in shape, as in the present case where small variations in the electronic state of the absorbing atoms due to environment fluctuations occur. Nevertheless, the Lorenzian shape was adopted in all curve fitting processes.) Any attempt to include a second resonance resulted in a line with parameters devoid of physical significance, for example, lines narrower than the Heisenberg natural width of the ^{119m}Sn nuclear decay. The resonance of samples 05(g), 06(g), and 10(g) corresponds to Sn atoms in substitutional positions in the a-Ge network.[9] Note that sample 10(g) contains a segregated layer of β-Sn at its outer surface. The

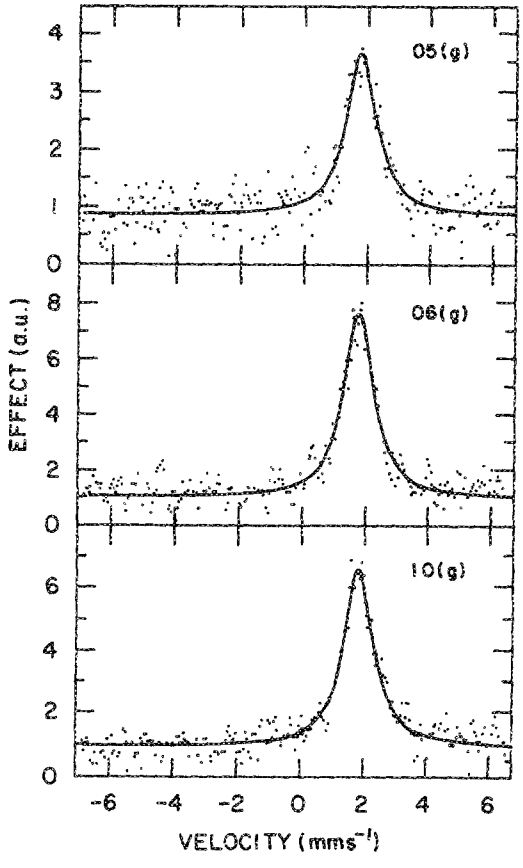

FIG. 3. ^{119}Sn conversion electron Mössbauer spectra from samples 05(g), 06(g), and 10(g). The solid lines represent the least-squares fitting of the experimental points with a single Lorenzian component. The corresponding isomer shifts and linewidth at half maximum are shown in Table II. The source was ^{119m}Sn in $BaSnO_3$.

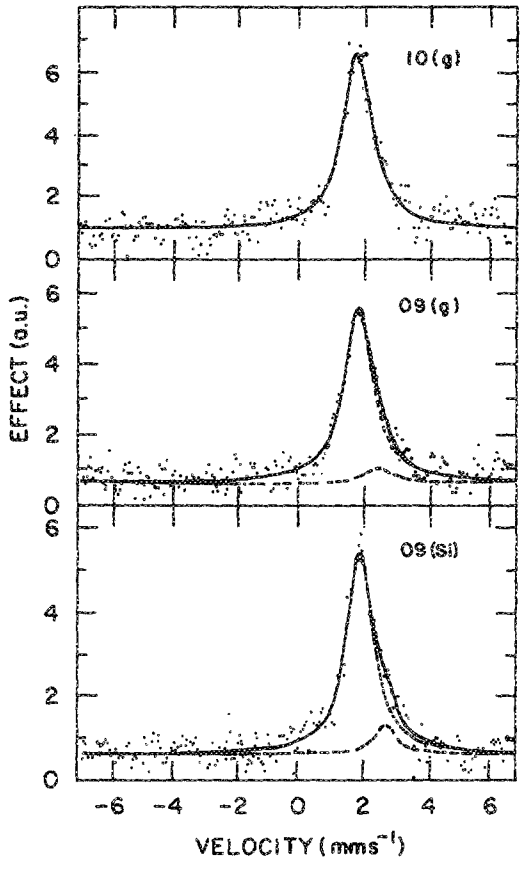

FIG. 4. Conversion electron Mössbauer spectra of a-Ge:Sn and a-Ge:Sn:H samples sputtered onto c-Si and Corning 7059 glass. The spectra correspond to high metal coverage of the Ge target, giving for sample 10(g) a Sn/(Ge + Sn) ratio of nearly 0.27. The solid lines represent the best least-squares fitting with one [No. 10(g)], and two [No. 09(Si) and No. 09(g)] Lorenzian components (dashed lines). The isomer shifts, linewidths, and respective areas are shown in Table II. The source was ^{119m}Sn in $BaSnO_3$.

metallic tin particles, however, do not produce any detectable Mössbauer signal.

Figure 4 shows the Mössbauer spectra of samples 09(g), 09(Si), and 10(g). The latter has been reproduced in this

TABLE II. Mössbauer fitting parameters of the spectra shown in Fig. 3 and those of Refs. 17 and 18.

Sample No.	Isomer shift (mm s^{-1})	Width at half maximum (mm s^{-1})	Area (%)	Observations
05(g)	2.02 ± 0.05	1.14 ± 0.08	100	a-Ge:Sn
09(g)	1.96 ± 0.05	1.09 ± 0.05	93	a-Ge:Sn
	2.56 ± 0.05	0.95 ± 0.08	07	
09(Si)	1.92 ± 0.05	1.00 ± 0.05	89	a-Ge:Sn
	2.71 ± 0.05	0.80 ± 0.08	11	
06(g)	1.96 ± 0.05	1.12 ± 0.06	100	a-Ge:Sn:H
10(g)	1.95 ± 0.05	1.11 ± 0.06	100	a-Ge:Sn:H
Ref. 17	1.90 ± 0.05	1.00 ± 0.05		Sn implanted in c-Ge
Ref. 18	2.00 ± 0.02	1.55 ± 0.06		Sn implanted in a-Ge
Ref. 18	2.14 ± 0.04	1.60 ± 0.10		Sn implanted in a-α tin

figure for comparison. It is worth remembering that all three samples have been deposited using the same target metal coverage conditions (see Table I for details on hydrogenation and β-Sn segregation). The best fit to the spectra of the 09 series requires a couple of resonances. The main one possesses an isomer shift corresponding to Sn atoms in a tetrahedral coordination, an indication that most tin atoms go substitutionally in the a-Ge network. The second line possesses a metallic character, with an isomer shift not much different of β-Sn ($\delta_{\beta-\mathrm{Sn}} = 2.56$ mm s^{-1}). Note that the second line appears only in unhydrogenated samples deposited under conditions of high Sn target coverage. The presence of hydrogen in the reaction chamber [No. 10(g)] inhibits this second resonance, another indication that it does not come from segregated β-Sn. Additional information is given by the linewidth at half maximum. Because of a 0.3-mm s^{-1} electric quadrupole splitting, β-Sn possesses a broad resonance[10] of the order of 1.3 mm s^{-1}. This is much broader than the width of the metallic line of samples 09(g) and 09(Si). We conclude that the second line detected in the 09 series corresponds to a Sn atom in the Ge network possessing a different chemical environment. In the Discussion section we give support to the assignment of this resonance to octahedrally coordinated Sn in the center of a relaxed Ge divacancy.

III. DISCUSSION

A. Difference in shape between the Mössbauer spectra of crystalline and amorphous semiconductors

Mössbauer investigations of tin in germanium have been carried out since many years ago. As the solubility of Sn in Ge is extremely low under equilibrium conditions,[11] these studies referred either to Sn as impurity atoms in the crystalline Ge lattice[12,13] or to supersaturated polycrystalline solid solutions of tin in germanium.[14,15] The ion implantation[16,17] technique has also provided interesting data on the possible bonding configurations of Sn in the crystalline Ge lattice, as well as on their subsequent evolution with annealing processes. In all the cases mentioned above, Mössbauer spectra show that the large majority of tin atoms in the Ge lattice have the sp^3 electronic configuration typical of Ge and α-Sn. Supersaturated solutions of tin in Ge may contain also segregated β-Sn. Ion implantation, on the other hand, is often accompanied by radiation damage of the host material.

More recently, Nanver, Weyer, and Deutch[18] studied the amorphous phases of silicon, germanium, and α-Sn by the Mössbauer emission spectroscopy of ion-implanted (radioactive ^{119m}Sn) films. The amorphous samples were vacuum evaporated at very high deposition rates (100–250 Å/s). According to Ref. 18, the differences between the Mössbauer spectra of crystalline and amorphous tetrahedrally bonded semiconductors are for the latter a 20% broadening in the spectral linewidth, a slight increase of the isomer shift of the main resonance, and a concomitant peak shape for this line, interpreted as being due to a sum of lines with different isomer shifts. Although the substitutional position is maintained for Sn atoms in the amorphous and the crystalline phases, the differences between their spectra was attributed to small local deviations from the ideal tetrahedral structure, most probably due to bond bending effects. Nanver and coworkers[18] found no dependence of the resonance parameters upon implanted dose in unhydrogenated samples. Our results, on the contrary, show (see Table II) that both the isomer shift increments and the line broadening effects depend on the tin and on the hydrogen concentration in the alloys and, therefore, are not specific characteristics of the amorphous phase. In the present amorphous samples, the isomer shift of the main line scans a velocity range between 1.92 and 2.09 mm s^{-1}. Similar considerations apply to the width at half maximum, which varies between 1.00 and 1.14 mm s^{-1}.

We believe that the differences between our results and those of Ref. 18 originate from differences in sample quality. The high evaporation rates used to prepare the implanted samples of Ref. 18 are known to produce a high density of voids in the amorphous Ge network. The subsequent ion bombardment would induce further degradation of the material homogeneity, which would persist even after long annealing times. Let us note that the annealing has to be made at relatively low temperatures if the amorphous phase is to be maintained.

The a-Ge:Sn and a-Ge:Sn:H samples discussed in the present paper were deposited under conditions ($T_s = 180$ °C; deposition rate, ~ 1 Å/s) yielding high-quality a-Ge:H.[19] They are believed to possess a less defective network than ion-implanted samples or fast-cooled supersaturated Ge-Sn solutions. The presence of hydrogen in the reaction chamber, on the other hand, introduces a new important difference with previous studies, for it is known that hydrogen atoms saturate dangling bonds, relieving the stresses inherent to rigid but nonideal tetrahedral networks. This being the case, it becomes understandable why the chemical environment of tetrahedrally bonded Sn atoms in an a-Ge:H network, as detected by Mössbauer spectroscopy, does not differ significantly from the one existing around impurity Sn atoms in substitutional sites of the crystalline Ge lattice. The isomer shift variations detected between different a-Ge:Sn and a-Ge:Sn:H samples should be interpreted as being due partially to compressional stresses produced by different atom sizes causing an increase in s-electron density at the nucleus of Sn atoms. Similar effects have been reported to occur in microcrystalline Ge-Sn supersaturated solid solutions.[15]

The results of Table II include several kinds of samples. Let us consider first samples 05(g) and 06(g), which were grown under the same deposition conditions, except for the presence of hydrogen in the sputtering atmosphere while depositing sample 06(g). Within the sensitivity limits of Rutherford backscattering spectrometry, no difference in the tin/germanium ratio was detected between them (see Fig. 1). Both samples display a Mössbauer spectrum which can be best fitted with just one Lorenzian line. The hydrogenation of the network produces two effects: (a) a considerable decrease of the isomer shift (see Table II) and (b) a small narrowing of the linewidth. In our opinion, both effects derive from a better topological ordering of the network, i.e., a decrease of average bond bending deviations and a reduction

of the internal stresses resulting from a reduced coordination number. Both are well-established facts in the technology of a-Si:H and a-Si:Ge:H alloy films. According to Table II, all Sn atoms of samples $05(g)$ and $06(g)$ are tetrahedrally coordinated and located in substitutional sites of the network. Obviously, this statement is only true within the sensitivity limits of the experimental technique, of the order of 5×10^{18} cm^{-3} in the present research. It is worth mentioning that such a value is well above the concentration of defects needed to degrade the transport properties in an amorphous semiconductor network. Consequently, the presence of undetectable defects having an influence on the electronic properties cannot be ruled out based on Mössbauer spectroscopy measurements only.

The beneficial action of hydrogen appears also in sample $10(g)$, in which the nonsegregated tin atoms seem to occupy tetrahedrally coordinated positions. The final isomer shift and the width of the resonance indicate a concentration and an environment not much different from sample $06(g)$ (15 at. % Sn). Summarizing, the Mössbauer spectra of samples $05(g)$, $06(g)$, and $10(g)$ give direct evidence on the beneficial action of hydrogenation in reducing the topological disorder. No other information can be extracted from these spectra concerning the structure of defects around tin atoms.

B. Metal segregation and the structure of defects

The other important group of samples refers to those prepared by rf sputtering a Ge target with a high tin coverage. First, we compare samples $09(g)$ and $10(g)$ and discuss the role of hydrogen in the tin segregation process. Second, an analysis of all three samples will be made and the nature of defects around tin atoms will be discussed.

Samples $09(g)$ and $10(g)$ were deposited onto glass under identical nominal conditions, except for the presence of hydrogen in the reaction chamber during the growth of sample $10(g)$. Here again the differences measured in all properties between both samples are attributable to the effects of hydrogenation. These differences are the following: RBS spectra clearly indicate Sn segregation at the surface of sample $10(g)$. X-ray diffraction inspection show the characteristic peaks of β-Sn. On the contrary, the RBS spectrum of sample $09(g)$ indicates a homogeneous sample. X-ray inspection of this sample does not give any evidence of internal β-Sn precipitation or segregation. Such a process may only exist below the x-ray sensitivity detection limit. It is curious to observe that a Mössbauer resonance having an isomer shift similar to β-Sn appears only in the nonsegregated sample. However, such a resonance has not the characteristic broadness of β-Sn. A likely explanation for these experimental facts follows.

β-Sn suffers from a very low recoil-free fraction at room temperature ($f=0.039$) compared to tetrahedrally coordinated Sn in a crystalline Ge lattice (0.23).[20] To our knowledge, no recoil-free fraction has been measured for substitutional tin in an a-Ge network. Assuming the recoil-free fraction of Sn in a-Ge to be similar to the above value for c-Ge, the resulting factor may reduce the β-Sn signal to a value below the present experimental sensitivity limit. This explanation is corroborated by the results of sample $10(g)$. In the fitting process of this sample, which shows a large fraction of β-Sn at its surface, a second line was fixed in the position corresponding to β-Sn and allowed to vary in intensity and width to obtain the best least-squares fit. The best fit was obtained for a line having a width of one-tenth of the Sn nuclear decay Heisenberg linewidth. We take this as a clear indication that our experimental setup is not sensitive enough to detect the resonance of segregated β-Sn.

The question of the origin of the second resonance remains open. We suggest that it originates from octahedrally coordinated tin, i.e., a chemical environment similar to β-Sn. The following discussion shows that the existence of this configuration is possible in the amorphous germanium network.

1. Elastic energy calculations

Let us consider a cluster of Ge atoms in the diamond structure such as the one shown in Fig. 5 and substitute the central atoms labeled 1 and 2 by a single Sn atom. Let us connect all the Ge-Ge nearest neighbors by bonds which behave elastically, that is, the potential between nearest atoms can be written as

$$v(i)=-\frac{3\alpha}{8d^2}\sum_i(\mathbf{r}_{il}\cdot\mathbf{r}_{il}-d^2)^2+\frac{3\beta}{16d^2}\sum_i\sum_j\left(\mathbf{r}_{il}\cdot\mathbf{r}_{jl}+\frac{d^2}{3}\right)^2. \quad (1)$$

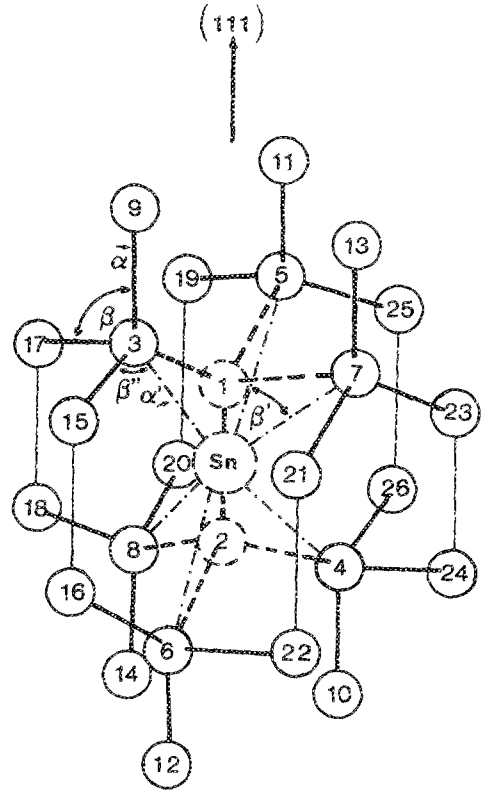

FIG. 5. Cluster of Ge atoms used to calculate elastic energy variations for a Sn atom in a Ge divacancy. The outer Ge atoms are held rigidly in their crystalline positions, while atoms 3–8 are allowed to relax. The central (α) and angular forces (β) tending to restore the tetrahedral or the octahedral bonding configurations are indicated.

This form of the potential produces central and angular forces that tend to restore the tetrahedral configuration. When Sn is bonded, it can be connected to the six nearest neighbors with a potential similar to (1), but with bond lengths and angles which correspond to the octahedral environment, that is,

$$v(0) = \frac{3\alpha'}{8d_0^2} \sum_j (\mathbf{r}_{oj} \cdot \mathbf{r}_{oj} - d_0^2)^2 + \frac{3\beta'^2}{16d_0^2} \sum_i \sum_j (\mathbf{r}_{io} \cdot \mathbf{r}_{jo})^2, \quad (2)$$

or connected to three sites with a tetrahedral potential. The parameters used in the model were extracted from the phonon density of states for Ge and the values for the Sn-Sn force constants from the ratio of the Raman modes $\nu_{Ge}/\nu_{Sn} = 1.596$. The initial positions of the atoms are those of Fig. 5 for Ge and Sn. The position of atom 1 can also be the initial site for the Sn atom. The relaxation process is done by calculating the displacements of all the seven interior atoms under the forces imposed by the bonding, that is,

$$\Delta \mathbf{r} = \mathbf{D}^{-1} \cdot \mathbf{F},$$

where $\Delta \mathbf{r}$ is a vector with 21 components which contains the displacements, $\mathbf{F}$ is the force calculated in the initial position, and $\mathbf{D}$ is the dynamical matrix, explicitly,

$$F_k(i) = -\frac{\partial v}{\partial x_k},$$

$$D_{kk'}(i) = \frac{\partial^2 v}{\partial x_k \partial x_{k'}}.$$

The results from the calculations are the following.

(i) When the Sn starts from the origin in an octahedral coordination, the final relaxed configuration is with the Sn remaining in the center and the neighbor Ge atoms relaxing symmetrically inwards. The dispersion of the Ge bonds is less than 1%, and the dispersion of the Ge angles is 9.4%, i.e., this octahedral configuration introduces less strain in the crystal network than the one usually found in pure amorphous Ge ($\sigma_\theta = 13\%$). The gain in elastic energy compared to the initial position is 55%, meaning that the final configuration is much more stable than the creation of three dangling bonds.

(ii) The local relaxed surrounding of the Sn atom is very similar to the one found in metallic β-Sn.

(iii) When the initial position of the Sn atom is off center, the system starts a damped oscillation around the same central octahedral configuration, although the displacement of the Ge atoms are not symmetric, approaching the Sn atom more than before and producing a large dispersion in the bonds and angles. This result can be connected to the preference for the off-center position in the crystal and not in the amorphous.

(iv) When Sn is forced to be in a tetrahedral coordination, the final position is off center, independent of the initial position, with substantial distortion of the bond lengths and angles ($\sigma_\theta > 15\%$). In the crystal, the rigidity of the diamond structure could allow for such high local distortion, but in the amorphous network, one can predict that it would be very difficult to find a tin atom in a tetrahedral environment adjacent to a vacancy.

2. Mössbauer and optoelectronic data

The above results on elastic energy minimization and the Mössbauer spectra of Figs. 3 and 4 suggest the following picture. Tin enters preferably in a tetrahedral substitutional position when the surrounding tissue has no defects. This configuration produces a local expansion of the network, since Sn is a bigger atom than Ge. Increasing amounts of Sn increase the stress in the network, inducing vacancy formation. Whenever a tin and a vacancy become adjacent, tin coordinates with six Ge atoms, producing a small contraction of the network locally. Note that the picture constitutes a less likely situation in a c-Ge lattice where, because of the host rigid structure, other bonding configurations for the impurity atom may be allowed. Accordingly, the amorphous network would tolerate larger amounts of tin than the crystalline Ge lattice, a conclusion in agreement with experiment.

The above description is also consistent with the results on hydrogenated material. It has been found experimentally that hydrogen induces metal segregation.[8] It is well known that atomic hydrogen passivates dangling bonds in amorphous semiconductors. In the present model, the satisfaction of Sn or Ge dangling bonds would inhibit the formation of the octahedral configuration and the concomitant relieving of the compressional stress. As a consequence, smaller amounts of tin are tolerated in the network for similar deposition temperatures. Infrared transmission measurements of the hydrogenated films do not indicate the existence of Sn—H bonds in a-Ge:Sn:H films, although large amounts of Ge—H are measured.[8] This is taken as an indication that the saturation of a pending Sn orbital by atomic H, representing an off-center Sn atom neighboring a vacancy, is not energetically favored in the amorphous network. It is worth stressing here that the lack of Sn—H absorption bands in the infrared spectra cannot derive from preferential attachment of hydrogen atoms to Ge dangling bonds. The Ge—H and Sn—H bond energies are 69 and 60.4 kcal/mol, respectively.[21] The small difference in the figures is not enough to explain the complete absence of Sn—H absorption bands in a-Ge:Sn:H films. According to our model, hydrogen cannot bond to a Sn pending orbital because this requires extra energy. A Mössbauer resonance attributable to Sn dangling bonds has not been detected in the amorphous samples, in agreement with the above considerations.

With respect to $BaSnO_3$, the chemical isomer shifts of ^{119m}Sn fall[22] in the velocity range -0.5 to $+4.5$ mm s^{-1}. Tin IV compounds give shifts below 2 mm s^{-1}, while a shift greater than 2.9 is indicative of tin in oxidation state II. Metals and alloys fall in the 1.3–3.0-mm s^{-1} region. The isomer shift of the second resonance measured in samples 09(g) and 09(Si) is consistent with a tin metallic orbital. The width of this resonance indicates the absence of any important electric field gradient, typical of chemical environments which do not possess cubic symmetry. This experimental finding suggests that the chemical environment of Sn in the center of

the relaxed Ge divacancy is more symmetric than in β-Sn, in accordance with the results of elastic energy minimization. Moreover, such an octahedral configuration embedded in a tetrahedral solid matrix will efficiently resonate. A large recoil-free fraction is to be expected because the possibility of a phonon emission during the process is inhibited by the difference in vibrational symmetry. As a consequence, such a defect will be easier to detect than β-Sn.

The small differences detected between the isomer shifts and widths of samples 09(g) and 09(Si) (see Table II) may originate from a different compressional stress in the network coming from different concentrations of substitutional tin in the alloy. We expect the compressional stress to be higher in sample 09(g) because the amount of tetrahedral tin is greater (no β-Sn segregation at the outer surface). The measured isomer shift and width of the main resonance is consistent with this assumption. Table II also indicates that the metallic segregation process is mainly done at the expense of substitutional tin in the network. This is an independent indication that the octahedrally coordinated Sn is firmly held in the defective site.

3. Transport properties

It is also an experimental fact that the addition of minute amounts of tin to the a-Ge:H network degrades the transport properties and kills the photoconductivity.[8] This is an indication that electronic states, related to tin, are introduced in the pseudogap. Conductivity-versus-temperature measurements show that an a-Ge:Sn:H alloy containing a few percent tin possesses a high-temperature activation energy a few tens of meV bigger than a-Ge:H. With the help of electron-spin resonance and infrared transmission techniques, Watkins[23] studied the tin-vacancy pair in crystalline Si. The conclusions of this study are that Sn atoms trap Si vacancies, the resulting tin-vacancy pair producing a donor level at $\sim E_v + 0.35$ eV. The analysis of the EPR spectrum leads to a model in which the tin atom resides in a position halfway between two normal silicon atoms in the center of a divacancy. The extension of this result to the octahedral configuration of tin in the a-Ge network discussed above is obvious. The octahedral configuration would give these electron states and will drive the formation of impurity bands which merge into the metallic bands of β-Sn. Let us note that tetrahedrally coordinated tin does not produce any state within the pseudogap.[24] Calculations of the electronic levels of the Sn atom in the center of a relaxed Ge divacancy are in progress.[25] Preliminary data give support to the present model.

Summarizing, the large majority of tin atoms go substitutionally in a-Ge:Sn:H films. The presence of atomic hydrogen inhibits the trapping of Ge vacancies by most Sn atoms. However, a small concentration of octahedrally coordinated tin, undetected by Mössbauer spectroscopy exists in the hydrogenated network. These defective sites produce states in the pseudogap of the alloy, degrading its transport properties.

IV. CONCLUSIONS

In this work a study of the defects around tin sites in amorphous Ge-Sn alloys is presented. Several new facts referring to the characteristics of the Mössbauer resonance of tin in the amorphous Ge network are reported. It is shown that in the alloy most of Sn atoms go substitutionally in the Ge network, as expected. The isomer shift and the width of the main resonance depend on the Sn content, on the presence of hydrogen in the film, and on the material quality. A second resonance has been identified in films having a large tin content. The analysis of its characteristics leads us to conclude that it corresponds to a chemical environment similar to the one found in β-Sn, i.e., to an octahedrally coordinated Sn. This defective configuration occurs because of trapping of Ge vacancies by Sn atoms. The final configuration is a Sn atom in the center of a relaxed Ge divacancy bonded to six neighboring Ge atoms. The existence of such a defect, which produces a local network contraction, is consistent with the following experimental findings: (a) Higher concentrations of tin are tolerated in chemically ordered amorphous networks than in crystalline ones. (b) The degradation of the transport properties is caused by minute amounts of tin because of new electronic states in the pseudogap. (c) Atomic hydrogen induces metal segregation. Octahedral tin is inhibited by the saturation of dangling bonds, and a higher compressional stress in the network results. The absence of Sn—H absorption bands in the infrared spectra of hydrogenated samples is also consistent with this picture.

The conclusions of the present study are far reaching, in the sense that they establish new limits to the technology of variable band-gap amorphous alloys. These limits are imposed by the most stable chemical configuration of foreign atoms at the normal and at the defective sites of elemental semiconductor networks. Let us remark that these defective sites are unavoidable in (overconstrained) tetrahedrally coordinated amorphous semiconductors. The present study shows that, in the case of column-IV heavier elements, a different coordination configuration having a metallic character appears to be stable in defective sites. The corresponding electron states degrade the optoelectronic properties of the alloys. Most of the present discussions and conclusions apply equally well to a-Si:Sn:H alloys in which experimental results indicate problems of similar nature.

ACKNOWLEDGMENTS

This research was partially supported by the Fundação de Amparo a Pesquisa do Estado de São Paulo (FAPESP) and the Conselho Nacional de Desenolvimento Científico e Technológico (CNPq), Brazil.

[1] Y. Kuwano and S. Tsuda, in *Amorphous Semiconductor Technologies and Devices*, edited by Y. Hamakawa (OHM–North-Holland, Tokyo, 1984).
[2] D. Anderson and W. Spear, Philos. Mag. **35**, 1 (1977).
[3] I. Chambouleyron, Appl. Phys. Lett. **47**, 117 (1985).
[4] See, for example, K. D. Mackenzie, J. R. Eggert, D. J. Leopold, Y. M. Li, S. Lin, and W. Paul, Phys. Rev. B **31**, 2198 (1985).
[5] A. H. Mahan, D. L. Williamson, and A. Madan, Appl. Phys. Lett. **44**, 220 (1984).
[6] R. J. Temkin, G. A. N. Connel, and W. Paul, Solid State Commun. **11**, 1591 (1972).
[7] I. Chambouleyron, F. C. Marques, J. P. de Souza, and I. J. R. Baumvol, J. Appl. Phys. **63**, 5596 (1988).
[8] I. Chambouleyron and F. C. Marques, J. Appl. Phys. **65**, 1591, (1989).

[9]L. K. Nanver, G. Weyer, and B. I. Deutch, Z. Phys. B **47**, 103 (1982).
[10]J. G. Stevens and V. E. Stevens, Eds., *Mössbauer Effect Data Index* (IFI/Plenum, New York, 1978).
[11]F. A. Trumbore, J. Electrochem. Soc. **103**, 597 (1956).
[12]P. P. Seregin, I. V. Nistiryuk, and F. S. Nasredinov, Sov. Phys. Solid State **17**, 1540 (1976).
[13]P. P. Seregin, S. R. Bakhchieva, M. G. Kekua, and A. V. Petrov, Sov. Phys. Solid State **21**, 718 (1979).
[14]R. N. Kuz'min and S. V. Nikitina, Sov. Phys. Solid State **13**, 3157 (1972).
[15]V. I. Lisichenko, N. N. Petrichenko, and A. A. Yakunin, Sov. Phys. Solid State **18**, 183 (1976).
[16]G. Weyer, A. Nylandsted-Larsen, B. I. Deutch, J. U. Andersen, and E. Antoncik, Hyperfine Interactions **1**, 93 (1975).
[17]G. Weyer, S. Damgaard, J. W. Petersen, and J. Heinemeier, Phys. Lett. **76A**, 321 (1980).
[18]L. K. Nanver, G. Weyer, and B. I. Deutch, Z. Phys. B **47**, 103 (1982).
[19]Sample 02 has a mobility-lifetime product of 5×10^{-9} cm^2/V at 1.25 eV photon energy and a light-to-dark conductivity ratio of 7×10^{-3} for a photon flux of 10^{16} cm^{-2} s^{-1}. The density of states in the pseudogap is estimated to approximately 3×10^{16} cm^{-3}, and the characteristic energy of the exponential absorption tail is 50 meV [estimated from photothermal deflection spectroscopy (PDS)]. The authors are indebted to Professor W. Paul, Harvard University, Cambridge, MA, and to Dr. M. L. Theye, Université de Paris VI, France, for photoconductivity and PDS data, respectively.
[20]J. W. Petersen, O. H. Nielsen, G. Weyer, E. Antoncik, and S. Damgaard, Phys. Rev. B. **21**, 4292 (1980).
[21]E. G. Rochow and E. W. Abel, *The Chemistry of Ge, Sn and Pb*, Vol. 14 of *Texts in Inorganic Chemistry* (Pergamon, London, 1975).
[22]N. N. Greenwood and T. C. Gibb, *Mössbauer Spectroscopy* (Chapman and Hall, London, 1971), Chap. 14.
[23]G. D. Watkins, Phys. Rev. **12**, 4383 (1975).
[24]R. A. Barrio, J. Tagüeña-Martinez, F. L. Castillo-Alvarado, and I. Chambouleyron (unpublished).
[25]R. A. Barrio, I. Chambouleyron, F. L. Castillo-Alvarado, and J. Tagüeña-Martinez (private communication).